Environmental Science
Water Research & Technology

ROYAL SOCIETY OF CHEMISTRY

PAPER

View Article Online
View Journal | View Issue

Cite this: *Environ. Sci.: Water Res. Technol.*, 2020, **6**, 2153

Understanding the composition and spatial distribution of biological selenate reduction products for potential selenium recovery†

Zhiming Zhang, [a] Yi Xiong,[a] Huan Chen[b] and Youneng Tang*[a]

Selenate is a common contaminant in agricultural drainage from areas with seleniferous soils. Microbes can convert selenate to elemental selenium nanoparticles, which may be recovered as a valuable resource. One challenge in the recovery of selenium from agricultural drainage is the coexistence of sulfate at very high concentrations. Studies have shown that sulfate may inhibit selenate reduction and lead to the precipitation of selenium sulfides, thus hindering the recovery of elemental selenium nanoparticles. It was found in this work that the hydraulic retention time (HRT) determined the effects of sulfate on selenate reduction by controlling the composition and spatial distribution of the selenium products in a H_2-based membrane biofilm reactor. At a HRT of 0.28 days, 99% of selenate was reduced to elemental selenium nanoparticles precipitated in the reactor and suspended in effluent, which was desirable for recovery. When the HRT was decreased to 0.14 days or smaller, selenium sulfides became the dominant particulate selenium product in the effluent. Interestingly, elemental selenium was always the dominant particulate selenium product in the biofilm regardless of HRT owing to further biological reduction of selenium sulfides to elemental selenium and sulfide. At HRTs of 0.28 and 0.14 days, famous selenate and selenite reducers such as *Rhodocyclaceae* (including *Azospira oryzae*) and *Rhizobium* sp. were enriched in the biofilm. Decreasing HRT to 0.07 days resulted in electron donor limitation, which further led to the biofilm dominated by *Desulfobulbaceae* that is well known for its ability to reduce sulfur and selenium oxyanions and the enrichment of sulfide-oxidizing bacteria.

Received 21st April 2020,
Accepted 26th June 2020

DOI: 10.1039/d0ew00376j

rsc.li/es-water

Water impact

Agricultural drainage is one of the major sources of selenium contamination. Selenate can be biologically converted to elemental selenium nanoparticles, which may be recovered as a valuable resource and a critical element, but selenium sulfides are common byproducts. This work identifies reactor operating conditions that lead to exclusive production of elemental selenium nanoparticles.

1. Introduction

Selenium exists in natural water environments at concentrations that vary from below 0.1 to 2000 μg Se per L.[1] Water impacted by agricultural drainage, power plant wastewater, and mining waste has higher selenium concentrations. For instance, its concentration is up to 4200 μg Se per L in the area of the San Joaquin Valley, which has been impacted by the agricultural drainage.[2] The high concentration of selenium in water needs to be treated due to its toxicity and bioaccumulation in food chains of the surrounding biosphere.[3] The maximum contaminant level (MCL) of 50 μg Se (total Se) per L in drinking water was established by the U.S. Environmental Protection Agency (USEPA).[4] Among its four oxidation states: selenate (Se,VI), selenite (Se,IV), elemental selenium (Se^0) and selenide (Se,-II), the two oxidized selenium forms are usually soluble and more toxic to biological systems due to their high mobility and bioavailability.[5,6] Conventional technologies for selenate and selenite removal are physicochemical processes such as ion exchange and reverse osmosis.[7–9] Microbial processes have been widely studied in recent decades and shown to be effective for selenate and selenite removal by converting them to elemental selenium nanoparticles, which can then be removed through processes such as filtration and precipitation.[10]

Studies in recent years yielded promising results for the potential recovery of elemental selenium produced in

[a] *Department of Civil and Environmental Engineering, FAMU-FSU College of Engineering, Florida State University, 2525 Pottsdamer Street, Tallahassee, Florida 32310, USA. E-mail: ytang@eng.famu.fsu.edu; Tel: +1(850)410 6119*
[b] *National High Magnetic Field Laboratory, Florida State University, 1800 East Paul Dirac Drive, Tallahassee, Florida 32310, USA*

† Electronic supplementary information (ESI) available: Related to this article can be found online. See DOI: 10.1039/d0ew00376j

microbial processes.[11,12] Selenium is a high-risk element vulnerable to supply restriction and other limitations,[13] a critical element for low carbon energy,[14] a borderline critical element of potential future high risk,[15] a critical E-tech element,[15] and a mineral deemed critical to U.S. National Security and the Economy.[16] Selenium is used as a valuable resource in various industrial fields such as glass production, alloys manufacture, synthesis of semiconductors, and development of batteries and solar cells.[5,11,12]

Sulfate, which is ubiquitous in water systems, directly affects the selenate removal and the elemental selenium recovery.[17,18] Various microbial species are able to simultaneously reduce selenate and sulfate, making sulfate as an antagonist for selenate reduction.[19–21] The analogous reactions for selenate and sulfate are due to their chemical similarities – both from group VIA of the periodic table.[19] Furthermore, the product of biological sulfate reduction (*i.e.*, HS^-) reacts with the intermediate of selenate reduction (*i.e.*, SeO_3^{2-}) to form selenium sulfides (*i.e.*, Se_nS_{8-n}), which are particulates.[22] Selenium sulfides may coexist with elemental selenium in the biological reactor and affect the downstream elemental selenium purification and recovery. Previous studies have greatly advanced the understanding of the interactions between sulfate and selenate in the microbial removal of selenate.[19,21] However, the following two questions, which affect the downstream selenium purification and recovery, are not answered. First, how are the particulate matters (*i.e.*, elemental selenium nanoparticles, selenium sulfides, and other potential particulate matters) distributed in a biological reactor (be suspended in treated water, precipitate in biofilm, or precipitate at the bottom of reactor)? Second, how does a key operating condition (*i.e.*, hydraulic retention time) affect the composition and spatial distribution of the selenium products in the reactor, and why? In addition, since selenium and sulfur are in the same chemical group in the periodic table, certain microbial species (*e.g.*, the famous sulfate reducing bacteria *Desulfovibrio desulfuricans*) can reduce both selenate and sulfate while others are able to reduce only one of them.[23] The third question to answer in this research is how the microbial community changes when the operating conditions vary and how this change affects the fate of selenate and sulfate in the system. The main objective of our study is to answer the three questions.

The effects of sulfate on selenate reduction are of particular importance for studying agricultural drainage because the concentrations of selenate and sulfate are simultaneously high. The concentration of sulfate in agricultural drainage varies from 780 to 2570 mg S per L and sometimes reaches 11 000 mg S per L.[24–27] For this reason, a synthetic agricultural drainage was used in our study. The H_2-based membrane biofilm reactor (MBfR) is one of the biological reactors that are efficient in selenate removal.[28,29] The MBfR uses H_2 gas as the electron donor to biologically reduce selenate to elemental selenium and was used in our study.[30]

2. Materials and methods

2.1 Configuration of the MBfR

The MBfR consisted of two cylindrical glass tubes (Fig. S1 in ESI†). One tube contained a bundle of ten 25 cm length polypropylene hollow fibers (Teijin Fibers, Ltd., USA). The fibers had an outer diameter of 200 μm and a wall thickness of 55 μm. One end of the fibers was sealed by knots while the other end was connected to an external gas cylinder, which supplied H_2 to the lumen of the fibers. The total volume of the MBfR was 30 mL. Simulated agricultural drainage was introduced into the system by a peristaltic pump (Model 07522-30, Masterflex L/S, Cole-Parmer, USA). To thoroughly mix the liquid in the two tubes, another pump (Model 77122-24, Masterflex C/L, Cole-Parmer, USA) was connected to the two tubes and recirculated the liquid between them at a flow rate of 29 L per day.

2.2 Operation of the MBfR

The composition of the synthetic agricultural drainage was made the same as typical agricultural drainages,[24,25,31] which contained Na_2SO_4 (6.66 g L^{-1}), $CaCl_2{\cdot}2H_2O$ (1.87 g L^{-1}), $MgCl_2{\cdot}6H_2O$ (2.37 g L^{-1}), $NaHCO_3$ (0.10 g L^{-1}), H_3BO_3 (0.08 g L^{-1}), Na_2SeO_4 (0.01 g L^{-1}), $KHCO_3$ (0.03 g L^{-1}), K_2HPO_4 (0.22 mg L^{-1}), KH_2PO_4 (0.26 mg L^{-1}), $FeCl_2{\cdot}4H_2O$ (0.64 mg L^{-1}), NH_4Cl (3.82 mg L^{-1}), $CuCl_2{\cdot}2H_2O$ (0.05 mg L^{-1}), $MnCl_2{\cdot}4H_2O$ (0.04 mg L^{-1}), $ZnCl_2$ (0.04 mg L^{-1}), $CoCl_2{\cdot}6H_2O$ (0.40 mg L^{-1}), $NiCl_2{\cdot}6H_2O$ (0.02 mg L^{-1}), $Na_2MoO_4{\cdot}2H_2O$ (0.13 mg L^{-1}), and $Na_2WO_4{\cdot}2H_2O$ (0.05 mg L^{-1}). The synthetic agricultural drainage was autoclaved and degassed by N_2 and CO_2 for 30 minutes to maintain an anaerobic condition and a pH of 7.0 ± 0.1. 10 mL inoculum and 20 mL of synthetic agricultural drainage were added into the MBfR. The inoculum was originally an activated sludge from a local wastewater treatment plant but anaerobically enriched in a sealed glass bottle by adding acetate and nitrate. After inoculation, the MBfR was operated in the batch mode for 24 hours and then changed to a continuous flow mode. The influent flow rates varied at 107, 214, and 428 mL per day at three stages, corresponding to hydraulic retention times (HRTs) of 0.28, 0.14, and 0.07 days, and selenate surface loading rates of 285, 570, and 1140 mg Se per m^2 per day, respectively. The hydrogen pressure was fixed at 5 psig.[30,32,33] Specific operating conditions for the three stages are summarized in Table S1.†

2.3 Sampling and chemical analysis

The reactor influent and effluent samples were typically taken once per week. The measurement of various selenium species is summarized in Fig. S2.† Selenate was the only selenium species in the influent ($[SeO_4^{2-}]_{in}$) and measured using ion chromatography (IC, Dionex Aquion ion chromatography system, Thermo Fisher Scientific, USA). For selenium species in the effluent, we first separated particulate selenium from dissolved selenium using centrifugation at 21 000 relative

centrifugal force for 30 min followed by filtration with a 20 nm pore size syringe filter. The dissolved selenium in the effluent ($[Se]_{dissolved,eff}$) was measured by a microwave plasma-atomic emission spectrometer (MP-AES, Model 4100, Agilent Technologies, USA). The dissolved selenate ($[SeO_4^{2-}]_{eff}$) and dissolved selenite ($[SeO_3^{2-}]_{eff}$) in the effluent were quantified using IC. The dissolved selenide in the effluent ($[Se^{2-}]_{eff}$) was estimated as $[Se]_{dissolved,eff} - [SeO_4^{2-}]_{eff} - [SeO_3^{2-}]_{eff}$. Particulate selenium in the effluent ($[Se]_{particulate\ in\ effluent}$) was calculated by subtracting $[Se]_{dissolved,eff}$ from the total selenium in the effluent ($[Se]_{total,eff}$), which was measured by MP-AES. Particulate selenium in the reactor ($[Se]_{particulate\ in\ reactor}$) was calculated by subtracting $[Se]_{particulate\ in\ effluent}$ from the total particulate selenium ($[Se]_{particulate}$), which was calculated by subtracting $[Se]_{dissolved,eff}$ from $[SeO_4^{2-}]_{in}$. Organic selenium was negligible according to measurement by the 3500-Se standard method.[34]

To further characterize the particulate selenium in the reactor and effluent, three sets of samples were taken during steady-state for each of the three stages. Those samples included 1) biofilm on fiber, 2) suspended particulates in the effluent, and 3) precipitated particulates at the bottom of the reactor. All samples were analyzed using scanning electron microscope (SEM, FEI Nova 400 Nano SEM, FEI, USA) coupled with Energy Dispersive X-ray (EDX). They were also analyzed using Raman spectroscopy (Renishaw, USA). Before being assayed by the SEM/EDX, the samples were pretreated by fixation, critical point drying and coating with iridium.[12]

Sulfate was the only sulfur species in the influent ($[SO_4^{2-}]_{in}$) and measured using IC during the three steady states. The dissolved sulfur species in the effluent at the three steady states were divided into sulfate ($[SO_4^{2-}]_{eff}$, measured by IC), sulfite ($[SO_3^{2-}]_{eff}$, measured by IC), and sulfide ($[S^{2-}]_{eff} = [H_2S] + [HS^-] + [S^{2-}]$, measured by the methylene blue method described in the 4500-S standard method).[34] The particulate sulfur species were simultaneously characterized when the particulate selenium species were characterized as described in the previous paragraph.

2.4 Biofilm sampling and microbial analysis

To track the changes in microbial communities for all three stages, a ~5 cm length fiber was cut off during the steady-state of each stage and then submerged in 10 mL autoclaved synthetic agricultural drainage for DNA extraction. The inoculum sample and the fiber samples were vortexed for 5 minutes and then centrifuged at 11 627*g* for 10 minutes at 4 °C. The supernatant fluid was discarded and the resulting cell pellets were preserved at −80 °C. Subsequently, total DNA from the cell pellets was extracted using a FastDNA SPIN for Soil kit (MP Biomedicals, USA) according to the manufacturer's instructions. The extracted DNA concentration was quantified with NanoDrop 2000 (Thermo Fisher Scientific, USA) prior to downstream sequencing. The DNA samples were analyzed with 16S rRNA gene-targeted amplicon sequencing by an Illumina MiSeq sequencer. Primer set 515F (GTGCCAGCMGCCGCGGTAA) and 806R (GGACTACHVGGGTWTCTAAT) used by Earth Microbiome Project was used in the 16S rRNA gene amplification, which follows a two-step PCR amplification protocol modified from Ionescu's report.[35] Raw sequences were joined, demultiplexed and then quality filtered using QIIME version 1.8. Sequences were then clustered into operational taxonomic units (OTUs) with a cutoff of 98% identity using USEARCH. Taxonomic annotations were assigned to each OTU using USEARCH and the Silva 132 reference database.[36]

3. Results and discussion

3.1 Composition and spatial distribution of selenium products in stage 1

Fig. 1 shows that selenate reduction started immediately at the beginning of stage 1 at an HRT of 0.28 days and a surface loading rate of 285 mg Se per m^2 per day. Selenate was reduced from the initial concentration of 4.2 mg Se per L to below the quantification limit (<0.02 mg Se per L) during steady-state of stage 1. As an intermediate, selenite initially accumulated to 2 mg Se per L on day 18; thereafter it gradually decreased to below the quantification limit (<0.02 mg Se per L). The dissolved selenium (selenate + selenite < 0.04 mg Se per L) in the effluent at steady state was below the drinking water standard set by USEPA (0.05 mg Se per L). Almost all selenate was converted to particulate selenium, of which approximately one third was suspended in the effluent and two-thirds was retained in the reactor (Fig. 1). The SEM images, EDX spectra, and Raman spectra in Fig. 2 consistently show that all particulate selenium (on fiber, in the effluent, and at the bottom of the reactor) was elemental selenium nanoparticles.

As shown in Table 1, the average difference for sulfate between the influent and effluent at the steady-state of stage 1 was 3.4 mg S per L. Almost all of them (*i.e.*, 3.4 mg S per L in Table 1) precipitated as calcium sulfate ($CaSO_4$) at the bottom of the reactor based on the following observations. First, the dissolved sulfur species other than sulfate was negligible in the effluent at steady state: sulfite in the effluent was below the quantification limit (<0.02 mg S per L) and the sulfide in the effluent was only 0.25 mg S per L (Table 1), compared to the influent sulfate concentratin of 1500 mg S per L. Second, $CaSO_4$ was the only particulate sulfur species observed. It was not found at the bottom of the influent bottle, but found at the bottom of the reactor (Fig. 2h and i), probably because of the slight pH increase (from 7.0 in influent to 7.4 in the reactor) and availability of microorganisms as crystallization nucleus.[37,38] The pH increase can be explained by the H^+ consumption in the biological reactions of selenate and sulfate (see eqn (1) and (2), from Rittmann and McCarty, 2012).[39] In summary, selenate was biologically reduced to elemental selenium

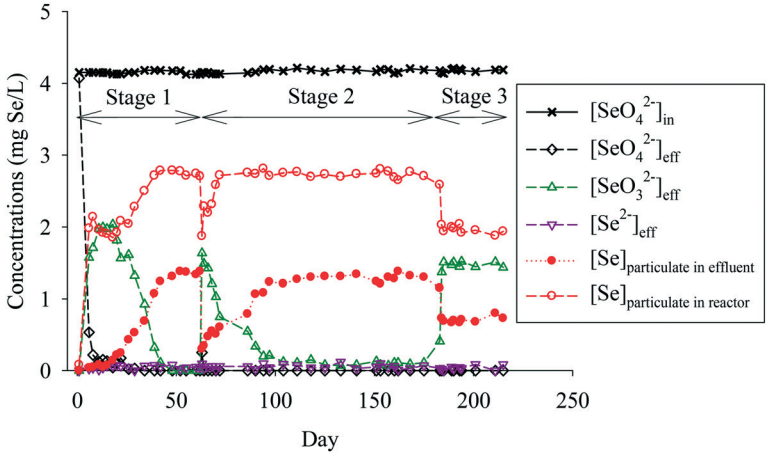

Fig. 1 Concentrations of selenium species at three stages with different HRTs.

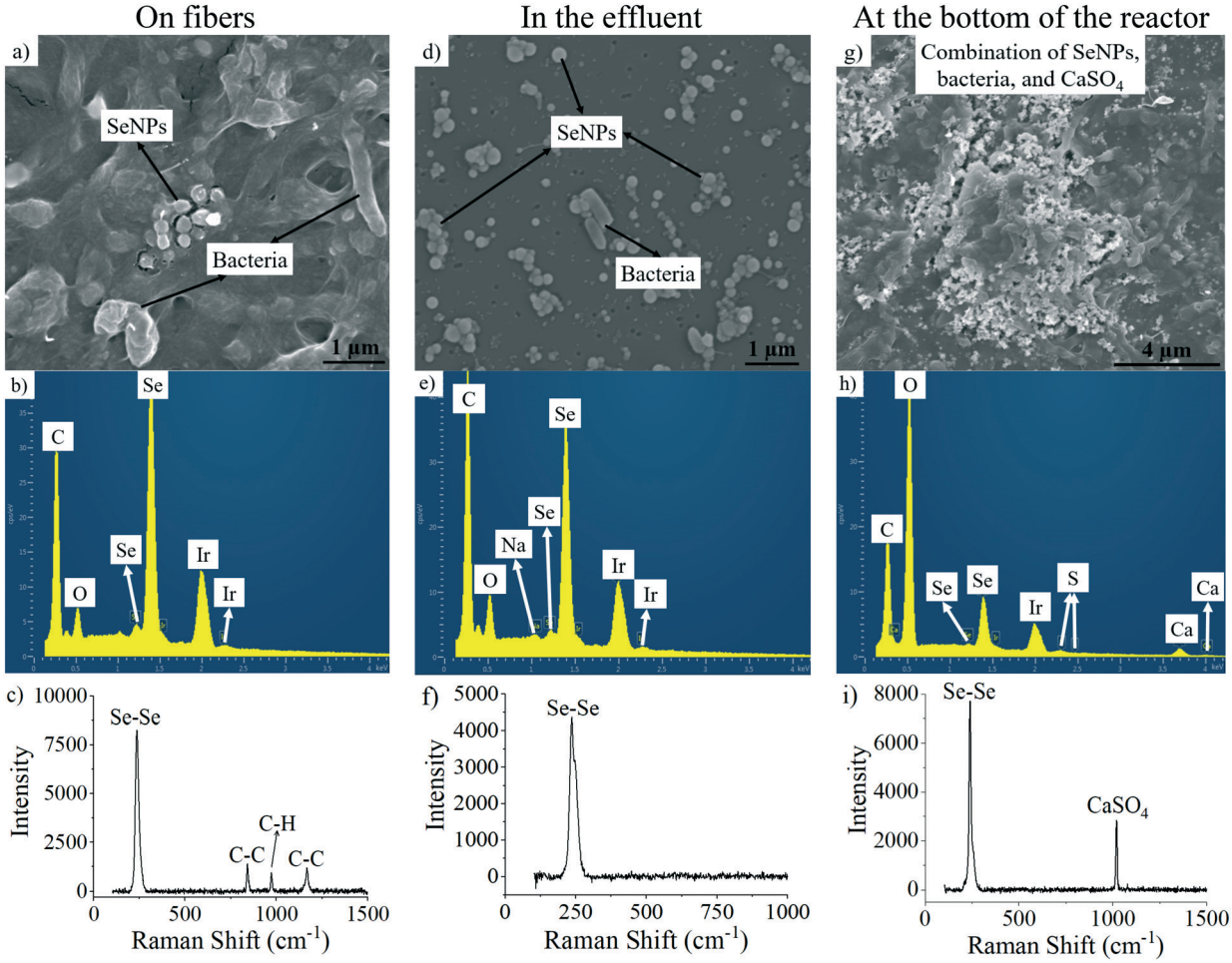

Fig. 2 Representative SEM images (the first row), EDX spectra (the second row), and Raman spectra (the third row) for particulates on fiber, in the effluent, and at the bottom of the reactor in stage 1. SeNPs = Elemental selenium nanoparticles.

nanoparticles in stage 1, while biological sulfate reduction was negligible. The difference between complete selenate reduction and negligible sulfate reduction can be explained by thermodynamics: the selenate reduction produces more energy (−71 kJ e^{-1}) than the sulfate reduction (−19 kJ e^{-1}),[40] and is thereby preferred by microbes as the electron acceptor. Metal sulfides were not formed at detectable levels in our study since we did not observe black precipitates in the reactor, and none of the Raman peaks in Fig. 2, 3 and 5 corresponded to metal sulfides.

Table 1 Concentrations of dissolved sulfur species during steady-state of the three stages

Stage	$[SO_4^{2-}]_{in}$ (mg S per L)	$[SO_4^{2-}]_{eff}$ (mg S per L)	$[SO_4^{2-}]_{in} - [SO_4^{2-}]_{eff}$ (mg S per L)	SO_4^{2-} removal rate (mg S per day)	$[SO_3^{2-}]_{eff}$ (mg S per L)	$[S^{2-}]_{eff}$ (mg S per L)
1	1529.5 ± 1.2	1526.2 ± 1.4	3.4 ± 0.3	0.36	<0.02	0.25
2	1526.6 ± 1.9	1524.3 ± 1.7	2.3 ± 0.3	0.49	<0.02	<0.05
3	1525 ± 2.9	1523.5 ± 2.8	1.5 ± 0.2	0.64	<0.02	<0.05

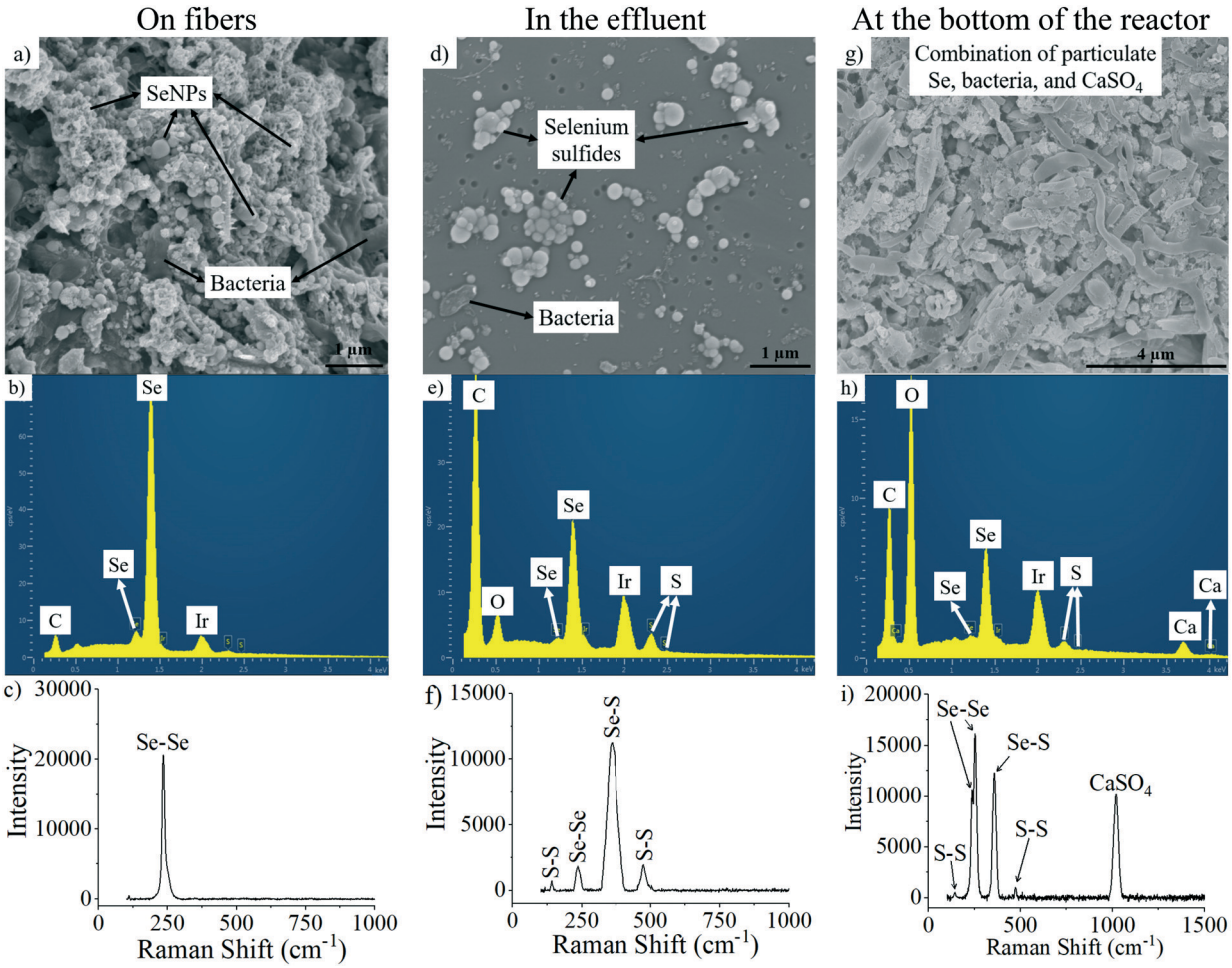

Fig. 3 Representative SEM images (the first row), EDX spectra (the second row), and Raman spectra (the third row) for particulates on fiber, in the effluent, and at the bottom of the reactor in stage 2. SeNPs = Elemental selenium nanoparticles.

$$0.5H_2 + 0.129SeO_4^{2-} + 0.045CO_2 + 0.011HCO_3^- + 0.011NH_4^+ + 0.258H^+ = 0.617H_2O + 0.011C_5H_7O_2N + 0.129Se^0 \quad (1)$$

$$0.5H_2 + 0.089SO_4^{2-} + 0.057CO_2 + 0.014HCO_3^- + 0.014NH_4^+ + 0.134H^+ = 0.045H_2S + 0.045HS^- + 0.486H_2O + 0.014C_5H_7O_2N \quad (2)$$

3.2 Composition and spatial distribution of selenium products in stage 2

As shown in Fig. 1 and 3, the composition and spatial distribution of selenium products in stage 2 were similar to those in stage 1, except for the following two changes. First, selenite accumulated to ~0.1 mg Se per L during the steady-state of stage 2; this was higher than the selenite concentration in stage 1 and the drinking water standard for total selenium set by USEPA. Second, selenium sulfides replaced elemental selenium nanoparticles as the dominant selenium products in the reactor effluent. We knew that selenium sulfides were the dominant products in the stage 2 effluent at steady state because all the particulates in the effluent contained sulfur and selenium per the EDX mapping spectra in Fig. 4, and the Raman spectra of these particulates in Fig. 3f corresponded to the common S–S, S–Se, and Se–Se bonds in selenium sulfides.[41,42] The different products in stage 2 compared to stage 1 suggests different selenate removal pathways: in stage 2, the increased selenate loading

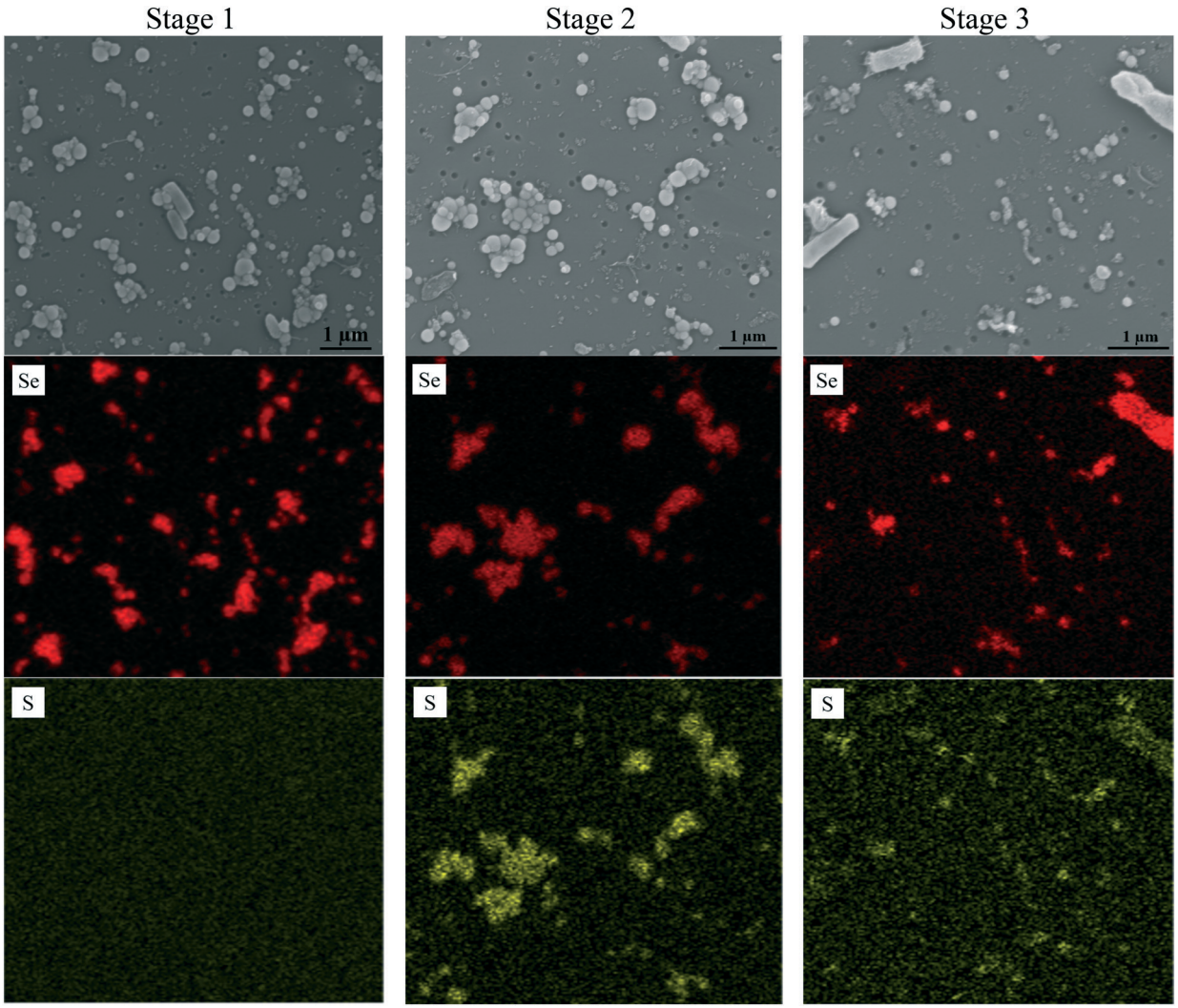

Fig. 4 SEM and EDX mapping spectra for particulates suspended in the effluent at the steady-state of the three stages.

(from 285 to 570 mg Se per m^2 per day) led to the accumulation of more selenite, which could react with sulfide to form selenium sulfides (reaction 1).[22,42]

$$n\mathrm{SeO_3}^{2-} + (8-n)\mathrm{HS}^- + (7n-8)\mathrm{H}^+ \rightarrow \mathrm{Se}_n\mathrm{S}_{8-n} + 3n\mathrm{H_2O} \quad (1)$$

Selenium sulfides were not observed in any locations in stage 1. The production of selenium sulfides in stage 1 was probably limited by unavailability of selenite. As shown in Fig. 1, there was negligible selenite (<the quantification limit of 0.02 mg Se per L) in the effluent of the reactor. Selenite, the intermediate of selenate reduction, did not accumulate in stage 1 as a result of a small selenate loading rate, but accumulated in stage 2 as a result of the doubled selenate loading rate. This correlation between selenite accumulation and selenate loading rate was consistent to other biological selenate studies.[12] It was also analogous to the well-known correlation between nitrite accumulation and biological nitrate reduction.[43] The reaction between selenite and sulfide probably proceeded until all sulfide was consumed in stage 2. This conclusion was based on the observation that selenite was 0.1 mg Se per L in the effluent, but sulfide was below the quantification limit of 0.05 mg S per L at the steady state of stage 2 (Table 1).

In stage 2, selenium sulfides were the dominant selenium products in the effluent, but elemental selenium nanoparticles were still the dominant selenium products in the biofilms on fibers (Fig. 3a–c, and 4). The difference might be caused by further biological reduction of selenium sulfides in the biofilm to elemental selenium and dissolved sulfide. The biofilm produced selenite and sulfide from biological selenate and sulfate reductions. The produced selenite and sulfide further abiotically reacted to form selenium sulfides per reaction 1 in both the biofilm and the bulk liquid of the reactor. However, the selenium sulfides in the biofilm could be biologically reduced to elemental selenium and sulfide, as described in Hageman *et al.* (2017),[44] but the selenium sulfides in the bulk liquid underwent no further reaction due to negligible biomass. Using SeS_2 as an example of selenium sulfides (reaction 2),

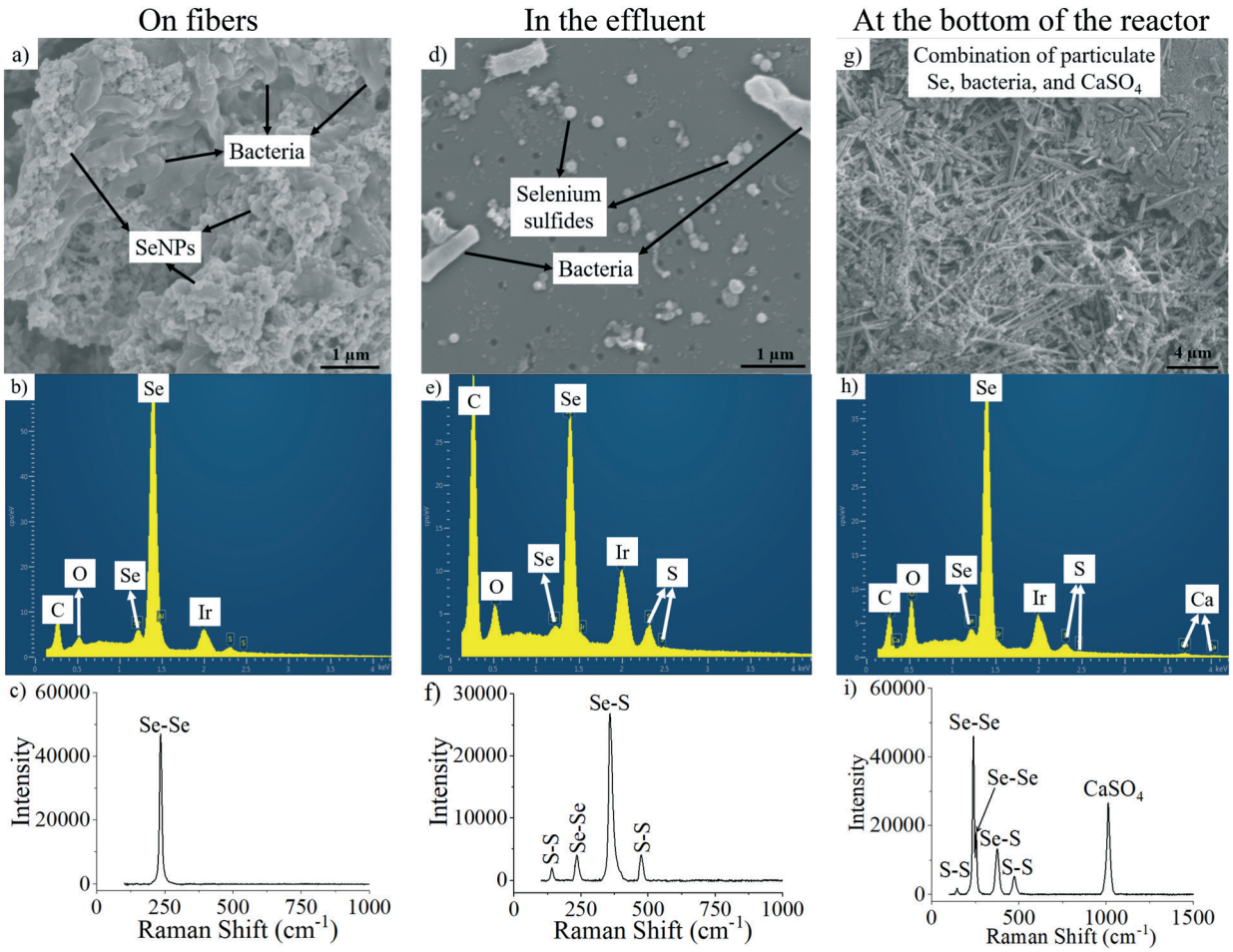

Fig. 5 Representative SEM images (the first row), EDX spectra (the second row), and Raman spectra (the third row) for particulates on fibers, in the effluent, and in reactor precipitate at stage 3. SeNPs = Elemental selenium nanoparticles.

the energy produced from this biological reaction (−23 kJ e^{-1}) was higher than the reaction between sulfate and hydrogen (−19 kJ e^{-1}).[40,43] Thereby this reaction likely occurred in the biofilm of our reactor.

$$2H_2(aq) + SeS_2 \rightarrow Se + 2HS^- + 2H^+ \quad (2)$$

Although the pH increased from 7.0 in the influent to 7.4 in the effluent, the small pH increase should not have led to abiotic breakdown of selenium sulfides to elemental selenium and elemental sulfur. Per Fig. 4, neither elemental selenium nor elemental sulfur was observed in the effluent. This is consistent with a previous study,[22] which showed stable selenium sulfides at pH = 7 and only a slight abiotic breakdown (<5%) of selenium sulfides at pH = 10 within 70 days.

3.3 Composition and spatial distribution of selenium products in stage 3

In stage 3, the selenate surface loading was further increased to 1140 mg Se per m^2 per day (HRT of 0.07 days). As shown in Fig. 1, 4 and 5, the composition and spatial distribution of selenium products in stage 3 were similar to those in stage 2, except for two changes. First, the selenite accumulation in the effluent at the steady-state of stage 3 further increased to ~1.5 mg Se per L, accounting for 36% of the total influent selenium (Fig. 1). Second, the medium ratio of selenium to sulfur for selenium sulfides in the steady-state effluent decreased from 1.7 in stage 2 to 1.2 in stage 3. The medium selenium to sulfur ratios were obtained from 60 and 35 EDX spectra of the selenium sulfides in stages 2 and 3, respectively. The accumulation of selenite was probably caused by three facts. First, the electron donor was limited since the required H_2 utilization flux at this stage was close to the theoretical maximum H_2 flux that could be supplied by the fiber at 5 psig (Table S2†). Second, microorganisms thermodynamically prefer selenate to selenite as the electron acceptor.[5] Third, the unavailability of sulfide (below quantification limit of 0.05) limited the consumption of selenite in the abiotic formation of selenium sulfides (reaction 1), which lead to accumulation of selenite. The change of selenium to sulfur ratio for selenium sulfides might be explained by the availability change of sulfide.

Sulfide was the limiting factor for reaction 1 in stages 2 and 3 since the sulfide concentration was below the quantification limit (Table 1). The sulfate removal rate was higher in stage 3 compared to stage 2 (Table 1), which might provide more sulfide for stage 3 compared to stage 2.

3.4 Changes in microbial communities

The microbial community in the inoculum (Fig. 6) was dominated by the genus of *Lactobacillus* (90.6% = 37.2% of *Lactobacillus* (unspecified) + 29.3% of *Lactobacillus kefiri* + 19.1% of *Lactobacillus casei* + 5% of *Lactobacillus brevis*). After the reactions reached a steady-state in stage 1 with H_2 as electron donor, *Lactobacillus* was outcompeted by other microbial groups such as *Rhodocyclaceae* (28.4% = 22.1% of unspecified *Rhodocyclaceae* + 6.3% of *Azospira oryzae*, a species in the family of *Rhodocyclaceae*), *Burkholderiaceae* (19.1% = 14.1% of genus *Massilia* + 5% of unspecified *Burkholderiaceae*), and *Alphaproteobacteria* (18.8% = 10.5% of *Rhizobium* sp. PY13 + 8.3% of unspecified *Alphaproteobacteria*). Among them, *Azospira oryzae* is well known for its ability to reduce selenate, and *Rhizobium* species is reported to reduce selenite.[45–47] Although detailed classification is not available for the unspecified species, those enriched microorganisms may also contribute to the reduction of selenium oxyanions (*i.e.*, selenate and selenite). For example, *Phaeobacter gallaeciensis* in the *Alphaproteobacteria* is reported to reduce both selenate and selenite.[48] *Thauera selenatis* in *Rhodocyclaceae* is reported to reduce selenate and selenite.[26] *Burkholderia cepacia* in *Burkholderiaceae* is also reported to reduce selenium oxyanions.[49]

In stage 2, the abundance of *Rhodocyclaceae* (41.6% = 39.4% of unspecified *Rhodocyclaceae* + 2.2% of *Azospira oryzae*) and *Rhizobium* sp. PY13 (14.3%) further increased (Fig. 6), probably due to the increasing selenate surface loading rate and subsequently the accumulation of more selenite, an electron acceptor for *Rhizobium*.[46] The sulfide generated from the biological reduction of sulfate and selenium sulfides might be used by sulfide-oxidizing bacteria (SOB), since microbes in *Rhodocyclaceae* (*e.g.*, *Dechloromonas agitata*) and *Burkholderiaceae* (*e.g.*, *Themothric azorensis*) are reported to use sulfide as the electron donor.[50,51]

Desulfobulbaceae was negligible in the first two stages (<0.1%), but became the dominant microbial group in stage 3 (44% = 35.3% of unspecified *Desulfobulbaceae* + 8.7% of *Desulfocapsa*, Fig. 6). *Desulfobulbaceae* is well known for its ability to reduce both sulfate and selenium oxyanions.[52,53] The common electron donor, H_2, was limiting in stage 3 (Table S2†), which probably favored the growth of microorganisms such as *Desulfobulbaceae* that can use two electron acceptors, selenate and sulfate. In addition, the high surface loading rates for selenate and sulfate in stage 3 (Table S1†) might promote the enrichment of *Desulfobulbaceae*. Consistent with the highest sulfate loading rate in stage 3, the sulfate removal rate (mg S per day) was also the highest in stage 3 (Table 1). Another notable change in the microbial community in this stage is the enrichment of *Hydrogenophilaceae* from <0.1% to 9% (Fig. 6). *Hydrogenophilaceae* is well known for its ability to use

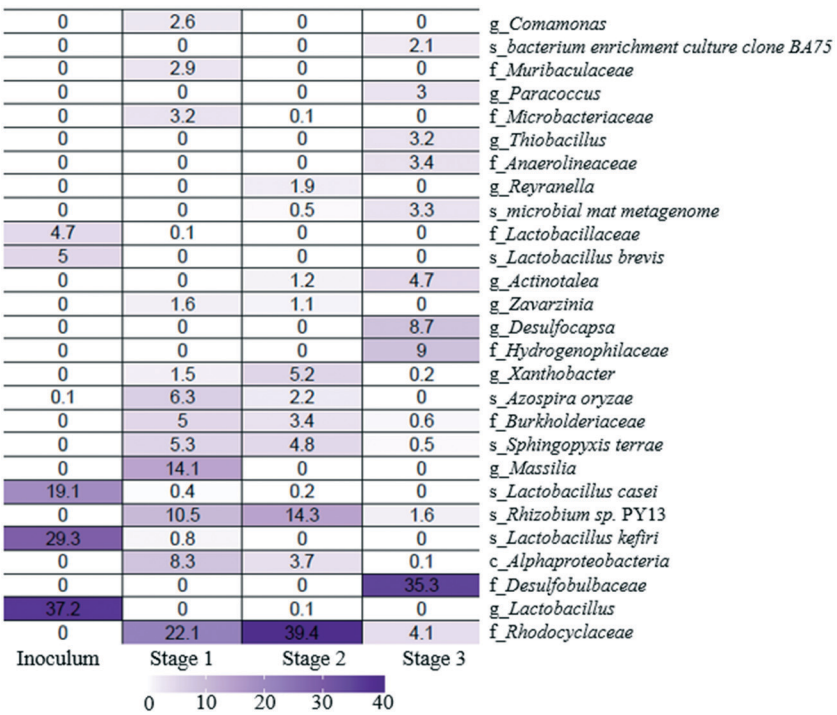

Fig. 6 The relative abundance (>2%) of various microbial groups in the inoculum and biofilms on fibers at the three stages. Notes: c = class, f = family, g = genus, and s = species.

reduced sulfur species (*e.g.*, sulfide) as electron donors.[50] They were enriched probably due to the hydrogen limitation as well.[54]

4. Conclusion

The HRT (or surface loading rate) affected the final products of biological selenate reduction in the agricultural drainage, which would further impact the selenium recovery. An HRT of 0.28 days or selenate surface loading rate of 285 mg Se per m^2 per day in the MBfR was desirable since selenate was removed to below the USEPA drinking water standard, elemental selenium nanoparticles were the only particulate selenium product, and the sulfate reduction was negligible (<0.2%). While $CaSO_4$ and bacteria co-precipitated with elemental selenium nanoparticles, $CaSO_4$ can be removed through dissolution in an acid solution, and bacteria may be removed through centrifugation or selective adsorption, resulting in recoverable elemental selenium nanoparticles. When the HRT decreased to 0.14 days or the selenate surface loading rate increased to 570 mg Se per m^2 per day, selenite accumulated and the selenium sulfides were formed, which would not only cause water quality concerns but also increase the impurity of the recovered elemental selenium.

Conflicts of interest

There are no conflicts of interest to declare.

Acknowledgements

This work was supported by a planning grant at Florida State University. Work performed at the National High Magnetic Field Laboratory ICR Facility is supported by the National Science Foundation Division of Chemistry through DMR-1644779 and the state of Florida. The authors greatly thank Dr. Eric Lochner for providing technical support in the SEM imaging, Dr. Jin Gyu Park at the High-Performance Material Institute at Florida State University for providing technical support in the Raman spectroscopy analysis, and Dr. Stefan J Green at the University of Illinois at Chicago for 16S rRNA sequencing.

References

1 F. M. Fordyce, Selenium deficiency and toxicity in the environment, in *Essentials of Medical Geology*, ed. O. Selinus, Springer, Dordrecht, 2013, pp. 375–416.
2 T. Presser and I. Barnes, *Dissolved constituents including selenium in waters in the vicinity of Kesterson National Wildlife Refuge and the West Grassland, Fresno and Merced Counties*, US Geological Survey, California, 1985.
3 S. J. Hamilton, Review of selenium toxicity in the aquatic food chain, *Sci. Total Environ.*, 2004, **326**, 1–31, DOI: 10.1016/j.scitotenv.2004.01.019.
4 United States Environmental Protection Agency (USEPA), *National Primary Drinking Water Standard*, Office of Groundwater and Drinking Water (4606M), U.S. EPA, Washington, D.C., 2003, EPA 816-F-03-016.
5 Y. V. Nancharaiah and P. N. L. Lens, Ecology and biotechnology of selenium-respiring bacteria, *Microbiol. Mol. Biol. Rev.*, 2015, **79**, 61–80, DOI: 10.1128/MMBR.00037-14.
6 Q. Zhou, Z. Yue, Q. Li, R. Zhou and L. Liu, Exposure to PbSe nanoparticles and male reproductive damage in a rat model, *Environ. Sci. Technol.*, 2019, **53**, 13408–13416, DOI: 10.1021/acs.est.9b03581.
7 T. Sandy and C. DiSante, prepared for North American Metals Council (NAMC), *Review of available technologies for the removal of selenium from water. Final Report*, 2010.
8 L. Moore and A. Mahmoudkhani, Methods for removing selenium from aqueous systems, *Proceedings Tailings and Mine Waste*, 2011.
9 S. Soda, M. Kashiwa, T. Kagami, M. Kuroda, M. Yamashita and M. Ike, Laboratory-scale bioreactors for soluble selenium removal from selenium refinery wastewater using anaerobic sludge, *Desalination*, 2011, **279**, 433–438, DOI: 10.1016/j.desal.2011.06.031.
10 D. T. Maiers, P. L. Wichlacz, D. L. Thompson and D. F. Bruhn, Selenate reduction by bacteria from a selenium-rich environment, *Appl. Environ. Microbiol.*, 1988, **54**, 2591–2593.
11 L. C. Staicu, E. D. Van Hullebusch and P. N. L. Lens, Production, recovery and reuse of biogenic elemental selenium, *Environ. Chem. Lett.*, 2015, **13**, 89–96, DOI: 10.1007/s10311-015-0492-8.
12 Z. Zhang, I. Adedeji, G. Chen and Y. Tang, Chemical-free recovery of elemental selenium from selenate-contaminated water by a system combining a biological reactor, a bacterium-nanoparticle separator, and a tangential flow filter, *Environ. Sci. Technol.*, 2018, **52**, 13231–13238, DOI: 10.1021/acs.est.8b04544.
13 T. E. Graedel, E. Harper, N. T. Nassar, P. Nuss and B. K. Reck, Criticality of metals and metalloids, *Proc. Natl. Acad. Sci. U. S. A.*, 2015, **112**, 4257–4262, DOI: 10.1073/pnas.1500415112.
14 R. Moss, E. Tzimas, H. Kara, P. Willis and J. Kooroshy, *Critical metals in strategic energy technologies. JRC-scientific and strategic reports*, European Commission Joint Research Centre Institute for Energy and Transport, 2011.
15 Natural Environment Research Council, *Sustainable use of natural resources*, 2013, URL http://www.nerc.ac.uk/research/funded/programmes/minerals/science-and-implementation-plan/.
16 K. J. Schulz, J. H. DeYoung, R. R. Seal and D. C. Bradley, *Critical Mineral Resources of the United States: Economic and Environmental Geology and Prospects for Future Supply, Geological Survey*, 2018.
17 M. B. Gerhardt, F. B. Green, R. D. Newman, T. J. Lundquist, R. B. Tresan and W. J. Oswald, Removal of selenium using a novel algal-bacterial process, *Res. J. Water Pollut. Control Fed.*, 1991, **63**, 799–805.
18 N. Quinn, T. Leighton, T. Lundquist, F. Green, M. Zárate and W. Oswald, Algal-bacterial treatment facility removes selenium from drainage water, *Calif. Agric.*, 2000, **54**, 50–56, DOI: 10.3733/ca.v054n06p50.

19 J. P. Zehr and R. S. Oremland, Reduction of selenate to selenide by sulfate-respiring bacteria: experiments with cell suspensions and estuarine sediments, *Appl. Environ. Microbiol.*, 1987, **53**, 1365–1369.

20 R. S. Oremland, J. T. Hollibaugh, A. S. Maest, T. S. Presser, L. G. Miller and C. W. Culbertson, Selenate reduction to elemental selenium by anaerobic bacteria in sediments and culture: biogeochemical significance of a novel, sulfate-independent respiration, *Appl. Environ. Microbiol.*, 1989, **55**, 2333–2343.

21 S. Hockin and G. M. Gadd, Removal of selenate from sulfate-containing media by sulfate-reducing bacterial biofilms, *Environ. Microbiol.*, 2006, **8**, 816–826, DOI: 10.1111/j.1462-2920.2005.00967.x.

22 N. Geoffroy and G. P. Demopoulos, The elimination of selenium (IV) from aqueous solution by precipitation with sodium sulfide, *J. Hazard. Mater.*, 2011, **185**, 148–154, DOI: 10.1016/j.jhazmat.2010.09.009.

23 F. A. Tomei, L. L. Barton, C. L. Lemanski, T. G. Zocco, N. H. Fink and L. O. Sillerud, Transformation of selenate and selenite to elemental selenium by Desulfovibrio desulfuricans, *J. Ind. Microbiol.*, 1995, **14**, 329–336, DOI: 10.1007/BF01569947.

24 J. A. Izbicki, *Chemical Quality of Agricultural Drainage Water Tributary to Kesterson Reservoir, Fresno and Merced Counties, California, January and August 1984*, Department of the Interior, US Geological Survey, 1989.

25 R. C. Squires, G. R. Groves and W. R. Johnston, Economics of selenium removal from drainage water, *J. Irrig. Drain. Eng.*, 1989, **115**, 48–57, DOI: 10.1061/(ASCE)0733-9437(1989)115:1(48).

26 J. M. Macy, S. Lawson and H. DeMoll-Decker, Bioremediation of selenium oxyanions in San Joaquin drainage water using Thauera selenatis in a biological reactor system, *Appl. Microbiol. Biotechnol.*, 1993, **40**, 588–594, DOI: 10.1007/BF00175752.

27 B. C. McCool, A. Rahardianto, J. Faria, K. Kovac, D. Lara and Y. Cohen, Feasibility of reverse osmosis desalination of brackish agricultural drainage water in the San Joaquin Valley, *Desalination*, 2010, **261**, 240–250, DOI: 10.1016/j.desal.2010.05.031.

28 Y. Wu, Y. Li, A. Ontiveros-Valencia, L. Ordaz-Díaz, J. Liu, C. Zhou and B. E. Rittmann, Enhancing denitrification using a novel in situ membrane biofilm reactor (isMBfR), *Water Res.*, 2017, **119**, 234–241, DOI: 10.1016/j.watres.2017.04.054.

29 Z. Zhang, G. Chen and Y. Tang, Towards selenium recovery: Biocathode induced selenate reduction to extracellular elemental selenium nanoparticles, *Chem. Eng. J.*, 2018, **351**, 1095–1103, DOI: 10.1016/j.cej.2018.06.172.

30 J. Chung, R. Nerenberg and B. E. Rittmann, Bioreduction of selenate using a hydrogen-based membrane biofilm reactor, *Environ. Sci. Technol.*, 2006, **40**, 1664–1671, DOI: 10.1021/es051251g.

31 Applied Algal Research Group, *The Algal-Bacterial Selenium Removal System for Treatment of Irrigation Drainage Water: Demonstration Facility Interim Studies*, 1999.

32 J. Chung, H. Ryu, M. Abbaszadegan and B. E. Rittmann, Community structure and function in a H_2-based membrane biofilm reactor capable of bioreduction of selenate and chromate, *Appl. Microbiol. Biotechnol.*, 2006, **72**, 1330–1339, DOI: 10.1007/s00253-006-0439-x.

33 Y. Tang, C. Zhou, S. W. Van Ginkel, A. Ontiveros-Valencia, J. Shin and B. E. Rittmann, Hydrogen permeability of the hollow fibers used in H_2-based membrane biofilm reactors, *J. Membr. Sci.*, 2012, **407-408**, 176–183, DOI: 10.1016/j.memsci.2012.03.040.

34 E. W. Rice, R. B. Baird, A. D. Eaton and L. S. Clesceri, *Standard Methods for the Examination of Water and Wastewater*, American Public Health Association/American Water Works Association/Water Environment Federation, Washington, DC, 2012.

35 D. Ionescu, W. A. Overholt, M. D. Lynch, J. D. Neufeld, A. Naqib and S. J. Green, Microbial community analysis using high-throughput amplicon sequencing, *Manual of Environmental Microbiology*, American Society of Microbiology, 4th edn, 2016, vol. 2.4.2, pp. 1–26, DOI: 10.1128/9781555818821.ch2.4.2.

36 R. C. Edgar, Search and clustering orders of magnitude faster than BLAST, *Bioinformatics*, 2010, **26**, 2460–2461, DOI: 10.1093/bioinformatics/btq461.

37 J. Shukla, V. P. Mohandas and A. Kumar, Effect of pH on the solubility of $CaSO_4{\cdot}2H_2O$ in aqueous NaCl solutions and physicochemical solution properties at 35 °C, *J. Chem. Eng. Data*, 2008, **53**, 2797–2800, DOI: 10.1021/je800465f.

38 R. Singh, H. Yoon, R. A. Sanford, L. Katz, B. W. Fouke and C. J. Werth, Metabolism-induced $CaCO_3$ biomineralization during reactive transport in a micromodel: Implications for porosity alteration, *Environ. Sci. Technol.*, 2015, **49**, 12094–12104, DOI: 10.1021/acs.est.5b00152.

39 B. E. Rittmann and P. L. McCarty, *Environmental biotechnology: principles and applications*, Tata McGraw-Hill Education, 2012.

40 R. Nerenberg and B. E. Rittmann, Hydrogen-based, hollow-fiber membrane biofilm reactor for reduction of perchlorate and other oxidized contaminants, *Water Sci. Technol.*, 2004, **49**, 223–230, DOI: 10.2166/wst.2004.0847.

41 J. W. Thomson, X. Wang, L. Hoch, D. Faulkner, S. Petrov and G. A. Ozin, Discovery and evaluation of a single source selenium sulfide precursor for the synthesis of alloy PbS_xSe_{1-x} nanocrystals, *J. Mater. Chem.*, 2012, **22**, 5984–5989.

42 Y. Tang, C. J. Werth, R. A. Sanford, R. Singh, K. Michelson, M. Nobu, W. Liu and A. J. Valocchi, Immobilization of selenite via two parallel pathways during in situ bioremediation, *Environ. Sci. Technol.*, 2015, **49**, 4543–4550, DOI: 10.1021/es506107r.

43 Y. Tang, M. Ziv-El, C. Zhou, J. H. Shin, C. H. Ahn, K. Meyer, D. Candelaria, D. Friese, R. Overstreet, R. Scott and B. E. Rittmann, Bioreduction of nitrate in groundwater using a pilot-scale hydrogen-based membrane biofilm reactor, *Front. Environ. Sci. Eng. China*, 2010, **4**, 280–285, DOI: 10.1007/s11783-010-0235-9.

44 S. P. W. Hageman, R. D. van der Weijden, A. J. M. Stams, P. van Cappellen and C. J. N. Buisman, Microbial selenium sulfide reduction for selenium recovery from wastewater,

J.Hazard. Mater., 2017, **329**, 110–119, DOI: 10.1016/j.jhazmat.2016.12.061.

45 M. Basaglia, A. Toffanin, E. Baldan, M. Bottegal, J. P. Shapleigh and S. Casella, Selenite-reducing capacity of the copper-containing nitrite reductase of Rhizobium sullae, *FEMS Microbiol. Lett.*, 2007, **269**, 124–130, DOI: 10.1111/j.1574-6968.2006.00617.x.

46 W. J. Hunter and L. D. Kuykendall, Reduction of selenite to elemental red selenium by Rhizobium sp. strain B1, *Curr. Microbiol.*, 2007, **55**, 344–349, DOI: 10.1007/s00284-007-0202-2.

47 W. J. Hunter, An Azospira oryzae (syn Dechlorosoma suillum) strain that reduces selenate and selenite to elemental red selenium, *Curr. Microbiol.*, 2007, **54**, 376–381, DOI: 10.1007/s00284-006-0474-y.

48 N. L. Brock, C. A. Citron, C. Zell, M. Berger, I. Wagner-Döbler, J. Petersen, T. Brinkhoff, M. Simon and J. S. Dickschat, Isotopically labeled sulfur compounds and synthetic selenium and tellurium analogues to study sulfur metabolism in marine bacteria, *Beilstein J. Org. Chem.*, 2013, **9**, 942–950, DOI: 10.3762/bjoc.9.108.

49 A. S. Templeton, T. P. Trainor, A. M. Spormann and G. E. Brown, Selenium speciation and partitioning within Burkholderia cepacia biofilms formed on α-Al_2O_3 surfaces, *Geochim. Cosmochim. Acta*, 2003, **67**, 3547–3557, DOI: 10.1016/S0016-7037(03)00212-6.

50 J. Orlygsson and J. K. Kristjansson, The Family Hydrogenophilaceae, in *The Prokaryotes: Alphaproteobacteria and Betaproteobacteria*, ed. E. Rosenberg, E. F. DeLong, S. Lory, E. Stackebrandt and F. Thompson, Springer, New York, 2014, pp. 859–868.

51 E. V. Odintsova, H. W. Jannasch, J. A. Mamone and T. A. Langworthy, Thermothrix azorensis sp. nov., an obligately chemolithoautotrophic, sulfur-oxidizing, thermophilic bacterium, *Int. J. Syst. Evol. Microbiol.*, 1996, **46**, 422–428, DOI: 10.1099/00207713-46-2-422.

52 G. Muyzer and A. J. M. Stams, The ecology and biotechnology of sulphate-reducing bacteria, *Nat. Rev. Microbiol.*, 2008, **6**, 441, DOI: 10.1038/nrmicro1892.

53 D. Y. Sorokin, T. P. Tourova, A. N. Panteleeva and G. Muyzer, Desulfonatronobacter acidivorans gen. nov., sp. nov. and Desulfobulbus alkaliphilus sp. nov., haloalkaliphilic heterotrophic sulfate-reducing bacteria from soda lakes, *Int. J. Syst. Evol. Microbiol.*, 2012, **62**, 2107–2113, DOI: 10.1099/ijs.0.029777-0.

54 A. Ontiveros-Valencia, C. R. Penton, R. Krajmalnik-Brown and B. E. Rittmann, Hydrogen-fed biofilm reactors reducing selenate and sulfate: Community structure and capture of elemental selenium within the biofilm, *Biotechnol. Bioeng.*, 2016, **113**, 1736–1744, DOI: 10.1002/bit.25945.